CORROSION AND PROTECTION OF NON-PATINATED, SULPHIDE- AND CHLORIDE-PATINATED BRONZE

KOROZIJA IN ZAŠČITA NEPATINIRANEGA, SULFIDNO- IN KLORIDNO-PATINIRANEGA BRONA

Živa Novak, Tadeja Kosec*

Slovenian National Building and Civil Engineering Institute, Dimičeva ulica 12, 1000 Ljubljana

The surface of bronze undergoes changes when it is exposed to a polluted atmosphere, and bronze should therefore be protected from this natural deterioration. The most common protective coating currently in use is Incralac, which includes toxic components and is reported to dissolve a few months after application. This work therefore investigates a fluoropolymer-based coating (FA-MS), and compares it to the protection offered by Incralac. Bronze samples (non-patinated, sulphide-patinated or chloride-patinated) were exposed to simulated urban rain for four months. The corrosion products formed were characterised using SEM/EDS and Raman analyses. To study the protection efficiency of the newly developed fluoropolymer coating (FA-MS) and Incralac protection, various electrochemical methods were used: measurements of open circuit potential linear polarisation and potentiodynamic measurements. Findings show that the FA-MS coating provides a protection efficiency of 71 % for chloride-patinated bronze and 99.5 % for sulphide-patinated bronze. Contact angles of the FA-MS samples were higher than those of the unprotected samples or the samples protected by Incralac, indicating better hydrophobic properties of the FA-MS coating.

Keywords: bronze, corrosion, SEM/EDS analyses, Raman spectroscopy, electrochemistry

Površina brona se z izpostavljenostjo onesnaženemu okolju spreminja, zato mora biti pred naravnim propadanjem zaščitena. Trenutno je najbolj pogosto uporabljen zaščitni premaz Incralac, ki vsebuje okolju škodljive snovi, hkrati pa poročajo, da po nanosu razpade že po nekaj mesecih. Na podlagi tega je bil v tej študiji raziskan zaščitni premaz na osnovi fluoropolimera (FA-MS), ter primerjava z Incralac premazom. Vzorci brona (ne-patiniran, rjavo-patiniran in kloridno-patiniran) so bili za štiri mesece izpostavljeni simulaciji deževnice v urbanem okolju. Tvorjeni korozijski produkti so bili nato označeni s pomočjo SEM/EDS in ramanske analize. Za študij učinkovitosti zaščite novo razvitega fluoropolimernega premaza (FA-MS) in Incralac zaščite smo uporabili različne elektrokemijske metode: meritve potenciala odprtega kroga, linearno polarizacijo in potenciodinamske meritve. Prav tako smo določili hidrofobnost z meritvami kontaktnih kotov in izmerili spremembe v barvi pred in po nanosu zaščite. Ugotovitve preiskav so, da FA-MS premaz nudi učinkovitost zaščite v vrednosti 71 % za kloridno patiniran bron in 99,5 % za sulfidno patiniran bron. Izmerjene vrednosti kontaktnih kotov vzorcev, zaščitenih s FA-MS prevleko, so bili višje kot pri nezaščitenih vzorcih in vzorcih, zaščitenih z Incralacom, kar kaže na izboljšane hidrofobne lastnosti FA-MS zaščite.

Ključne besede: bron, korozija, SEM/EDS analiza, Raman spektroskopija, elektrokemija

1 INTRODUCTION

Patinas form on bronze surfaces due to exposure to the atmosphere. They consist of different copper corrosion products in various colours, usually reddish, turning to black, green and blue.[1]

Some natural patinas are referred to as 'noble rust', due to their artistic look and stability, protecting the bronze from further corrosion, while others are known as 'bronze disease', causing a constant loss in the material.[1,2] Cuprite (Cu_2O), for example, successfully protects bronze from further corrosion, while in a chloride-rich atmosphere, cuprous chloride (CuCl) is formed, which continuously releases chlorides that react with copper, causing cyclic pitting corrosion and the formation of atacamite.[1–3] Similarly, in the presence of SO_4^{2-}, brochantite usually forms, which, after longer periods of exposure to acidic water, transforms into antlerite.[4] In contrast to the formation of natural patinas, artificial patination is an important final stage in the process of producing bronze artwork.[5] It both represents the age of an artefact and adds to its value[6], so different methods to create artificial patination have been established.

The stability of products formed on bronze can be determined from the thermodynamic properties of each mineral, more specifically through the measurement of the Gibbs free energy.[7] Artificial and natural patinas are composed of many different copper minerals; the stability of a patina can be spectroscopically investigated after long periods of immersion in a solution, while the stability of the corrosion products formed on bronze can be measured through various electrochemical techniques. Corrosion resistance can therefore be determined with linear polarisation, electrochemical impedance spectroscopy, or potentiodynamic curves. Raman, FTIR, SEM/EDS or XRD analysis can be used to identify the minerals formed. The cross-sectional microstructure of a sample can be observed using the FIB (focused ion

*Corresponding author's e-mail:
tadeja.kosec@zag.si (Tadeja Kosec)

beam)-SEM technology, or with an optical microscope after polishing and etching, and the thickness of the patina layer or protective coating can be determined. The composition and binding of the protective coating can also be determined with XPS spectroscopy.[1]

Since, in essence, patination is a form of corrosion, many different coatings have been studied over the years, with the desire to retain the colours of an artefact while simultaneously protecting it.[8] The coating most commonly used within the field of conservation is Incralac, which is composed of Paraloid B-44 with a BTA inhibitor,[9,10] and has been reported to deteriorate over time.[9,11,12] The use of different fluoropolymers and waxes has also been explored,[9,13–15] and different inhibitors can also be added.[15,16] It is, however, important to be aware of a potential change in the colour following the application of a coating. Potential protective coatings must be suitably characterised and electrochemically tested. In addition to electrochemical evaluation, the characteristics investigated usually include changes in the contact angle, colour changes, hardness, information regarding the thickness of the coating, and the transmittance of UV light.

In this paper, bare CuSnZnPb and bronze with two different artificial patinas – brown sulphide and green chloride – were exposed to a solution of artificial urban rain for approximately four months in order to study the development of corrosion over time. The corrosion products formed were identified with SEM/EDS and Raman spectroscopy.

The protection efficiency of the FA-MS coating on bare bronze, brown-patinated bronze and green-patinated bronze was evaluated electrochemically. The hydrophobicity and differences in colour between pre- and post-application were also studied. The results obtained were compared to those of the commercial coating, Incralac.

2 EXPERIMENTAL PART

2.1 Bronze

A leaded bronze plate representative of quaternary bronze[17] (composition in w/%: 5.28 Sn, 3.84 Zn, and 2.71 Pb, with Cu to balance) was cut into discs with a 15-mm diameter. The composition of the quaternary CuSnZnPb bronze studied was obtained with an optical emission spectrometer (OES – Oxford Instruments, 2011).

2.2 Surface preparation – patination

The surface of the bronze was prepared for tests in three different ways (bare bronze, sulphide-patinated bronze and chloride-patinated bronze), as shown in **Figure 1**. All discs were first abraded with 1200 grit SiC paper and ultrasonically cleaned for 3 min in ethanol. 3 w/% K_2S solution was used for the brown sulphide

patination.[15] The bronze was first heated, then the solution was applied over the hot surface with a brush a total of three times. The sulphide-patinated samples were then washed with deionised water and aged at room temperature for 24 h. The green chloride patination was applied over the sulphide-patinated samples at 45 °C. The solution used for the chloride patina was composed of 2 g NH_4Cl, 2 g NH_4HCO_3 and 6 mL water. Immediately before the application, the solution was diluted with additional 50 % volume of deionised water. These samples were then placed into a sealed plastic bag containing a cotton pad soaked in water in order to create a very humid environment, and left for 24 h.

2.2 Composition and application of the protective coatings

Two different coatings were applied over the bare and patinated bronze samples. Specifically, Incralac, a commercial protective coating commonly used in restoration work, was diluted with n-butyl acetate and compared to the newly developed fluoropolymer coating combined with an adhesion promotor. 8.4 mg of solution was applied to each sample, then samples were dried at room temperature for at least 1 h.

The fluoropolymer (FA-MS) protective coating consisted of 5 % FA and 10 % MS in an equal solvent mixture of n-butyl acetate and diethyl succinate, as previously reported.[14] Approximately 2–3 mg of FA-MS was added to the 15-mm-diameter bronze discs, adding approximately 1.1–1.70 g/m² of dry mass. The samples were then dried at room temperature for at least 1 h followed by further 24 h in a drying chamber at 40 °C.

2.3 SEM/EDS and Raman analyses

The bare, brown-patinated and green-patinated bronze samples were then immersed in an artificial rain solution composed of 68.6 mg/L SO_4^{2-}, 28.7 mg/L Cl^- and 94.3 mg/L NO_3^-, simulating 100 times the concentration of urban Ljubljana rain. After 128 d of immersion, a SEM/EDS analysis was performed on the samples using a Jeol JSM IT500 LV (Japan, 2019), observed at different magnifications using a 20 keV excitation signal.

Raman spectroscopy was also conducted at this time in order to study any corrosion products on the unprotected samples of bronze, either non-patinated or covered
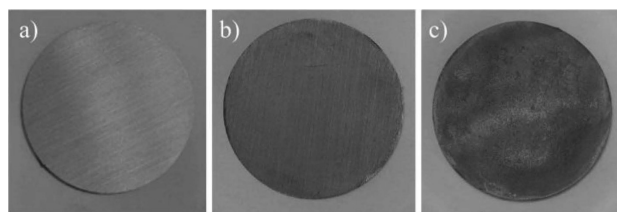
Figure 1: Three different 15-mm-diameter samples of the bronze studied: a) bare bronze, b) sulphide-patinated bronze, c) green chloride-patinated bronze

with a sulphide or chloride patina. A LabRAM Horiba Yvon 800HR was used for measurements, using a laser wave length of 532 nm at 10 % maximal power (100 mW). Spectra were collected in a range of 50–4000 cm^{-1}. The spectra presented are without background subtraction.

2.4 Electrochemical tests

An electrochemical investigation was performed using a Gamry 600+ potentiostat with a three-electrode system cell. The electrochemical solution was artificial urban rain with a composition of 685.7 mg/L SO_4^{2-}, 287.0 mg/L Cl^- and 943.2 mg/L NO_3^-, from sodium salts, simulating 1000 times the concentration of a Ljubljana district.[18] The samples were placed in a teflon holder with a surface area of 0.785 cm^2 exposed to the solution. An Ag/AgCl reference electrode and a graphite working electrode were used for the tests. The samples coated with Incralac were measured at least twice, while a minimum of three measurements were carried out for the remaining samples.

Firstly, open circuit potential (OCP) was measured for 3600 s, followed by linear polarisation resistance measurements (LP) within ± 20 mV of the OCP, carried out at a scan rate of 0.1 mV/s. Finally, potentiodynamic measurements were carried out from –0.25 V below E_{corr} to approximately 0.4 V above the reference electrode potential, at a scan rate of 0.167 mV/s.

The corrosion resistance values, R_p, obtained were further used to calculate the protection efficiency (PE) from Equation (1) where R_p refers to the unprotected sample and R'_p to the sample with protection:

$$PE \, / \, \% = \left(1 - \frac{R_P}{R'_P}\right) \cdot 100 \, \% \qquad (1)$$

2.6 Contact-angle measurement

Contact angles were measured using the FTA 1000 DropShape Instrument B FrameSystem (First Ten Angstroms, Newark, USA). At least three measurements were made on each sample before and after the application of the protective coatings, using a 2-μL droplet of deionised water. Due to a high variance in the results, the standard deviation of measurements was also provided.

2.7 Colour variations

Colour variations were specified with the CIEL*a*b* system through the use of an i1 colourimeter (X-Rite, USA) instrument prior to and following the application of the protective coatings. Each sample was measured three times, then the average and total colour differences, ΔE*, were calculated using Equation (2):

$$\Delta E_a^* = \sqrt{(\Delta L^{*2} + \Delta a^{*2} + \Delta b^{*2})} \qquad (2)$$

When the value of ΔE_{ab}^* is higher than three, the difference in colour can be distinguished with the naked eye, which should be taken into consideration when protecting bronze statues.

3 RESULTS AND DISCUSSION

3.1 Characterisation of corrosion products

Following the 128-d exposure to simulated urban rain, corrosion products were identified using SEM-EDS and Raman spectroscopy, the results of which are shown in **Figures 2** and **3**, respectively.
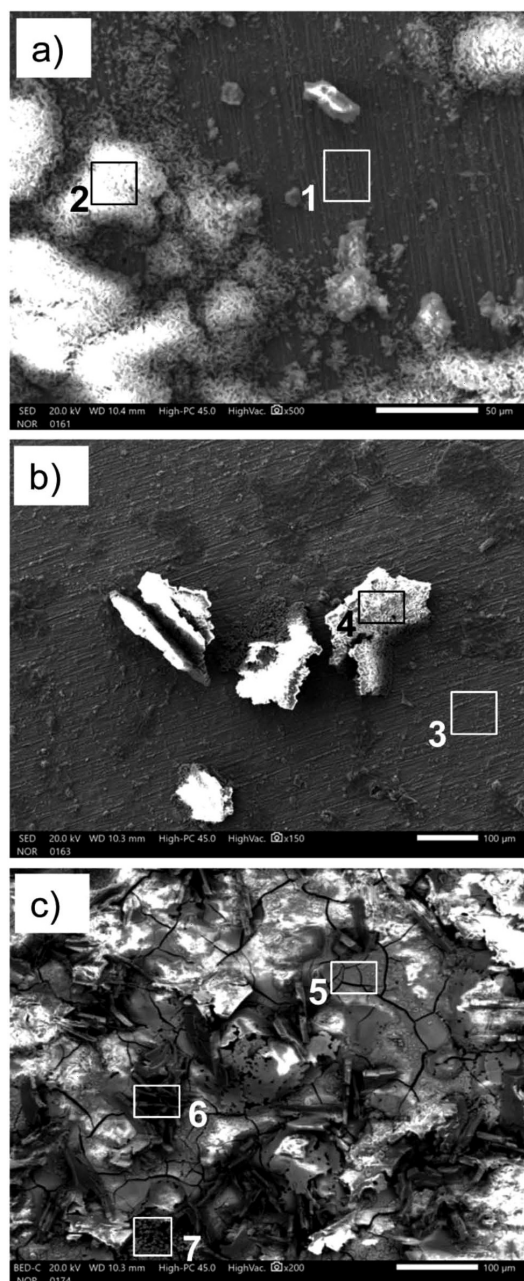
Figure 2: SEM images and areas of the EDS analysis following 128 d of immersion in the artificial urban rain: a) bare bronze, b) sulphide-patinated bronze, c) chloride-patinated bronze

Table 1: EDS analysis of the areas following 128 d of immersion in the artificial urban rain

Sample	Area	Cu	Sn	Zn	C	O	S	Cl	impurities
Bare bronze	1	63.9	7.18	2.45	11.2	8.3	6.5	—	0.44
	2	48.0	—	0.82	8.02	32.8	10.3	—	balance
Sulphide-patinated bronze	3	62.4	2.3	—	13.3	13.6	7.05	0.95	0.37
	4	45.8	—	0.49	9.92	36.7	7.06	—	balance
Chloride-patinated bronze	5	54.0	—	1.11	12.1	20.7	3.50	8.23	0.39
	6	55.0	—	—	8.90	30.9	4.65	0.52	0.01
	7	55.9	—	—	11.2	21.1	2.1	9.72	balance

Two typical morphologies were observed on the bare bronze after 128 d of immersion in the artificial rain, as shown in **Figure 2a**. The area marked as 1 represents a part of the surface where no visible corrosion products were formed, but visible grinding marks were present. The EDS analysis (**Table 1**, area 1) confirmed the presence of cuprous oxide, with sulphur also detected. Area 2 is a typical conglomerate of fine needle-like crystals with smaller and denser clusters. The EDS analysis (**Table 1**, area 2) showed the presence of Cu, O and S.

Figure 3: Raman spectra after 128 d of immersion in simulated urban rain: a) and b) bare bronze, c) and d) sulphide-patinated bronze, e) and f) chloride-patinated bronze

In general, the flattest part of sulphide bronze consists of Cu, Sn, C, O and S (**Table 1**, area 3), as can be seen in **Figure 2b**. Isolated plate-like crystals formed on the surface, which also contained Cu, O and S (**Table 1**, area 4).

Three different morphologies of corrosion products were detected on the chloride-patinated bronze following 128 d of exposure to urban rain, as shown in **Figure 2c**. The flat, cracked area at point 5 represents the base layer, which contains a higher amount of Cl (**Table 1**, area 5). Islands of flat patches are distributed across the surface. The EDS analysis confirmed the presence of Cu, O, S and Cl in area 6 (**Table 1**, area 6). Tiny clusters can also form on the surface, as visible at point 7. The elemental composition of these clusters is similar to that for area 5.

Further characterisation was conducted with Raman spectroscopy, the spectra of which are shown in **Figure 3**, with the peaks identified.

The Raman spectrum for area 1 of the bare bronze (defined in **Figure 2a**) revealed the presence of cuprite, Cu_2O (**Figure 3a**). The Raman spectrum consisted of narrow bands at 91 cm^{-1} and 213 cm^{-1} and broad bands positioned at 517 cm^{-1} and 626 cm^{-1}, as reported previously.[20,21]

The Raman spectrum for area 2 (as presented in **Figure 2a**) consisted of characteristic bands at 211 cm^{-1} and 354 cm^{-1}, a triplet at (454, 514 and 604) cm^{-1}, a very strong band at 963 cm^{-1}, and weak bands at 1069 cm^{-1} and 1185 cm^{-1}. Broad bands were further observed at 3453 cm^{-1} and 3536 cm^{-1}, indicating the presence of posnjakite, while the narrow band at 3572 cm^{-1} shows that brochantite was also present (see **Table 2**).

The Raman spectrum for area 3 (as presented in **Figure 2b**) consisted of narrow bands at (211, 434, 465, 521 and 610) cm^{-1}, showing the presence of cuprite, in addition to the bands at 281 cm^{-1} and 395 cm^{-1} characteristic of Cu_2S, representing the brown patina resulting from the artificial patination.[22]

The Raman spectrum of the corrosion product in area 4 (identified in **Figure 2b**) consisted of the bands positioned at (441, 503 and 611) cm^{-1}, a very strong band at 972 cm^{-1}, weak bands at (1065, 1112 and 1147) cm^{-1}, and broad bands at (3266, 2423 and 3550) cm^{-1}, indicating the presence of brochantite (**Table 2**).
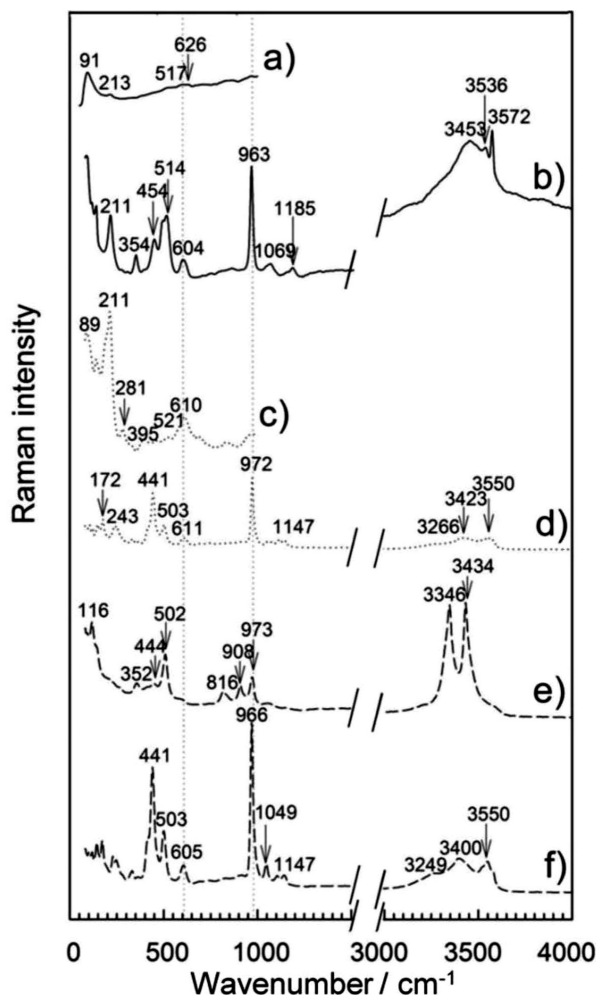
Following 128 d of exposure, the Raman spectrum of the chloride-patinated bronze showed the following characteristic bands: (352, 444 and 502) cm^{-1}, a triplet at (816, 908 and 973) cm^{-1} and two bands at 3346 cm^{-1} and 3434 cm^{-1}. This spectrum was identified as atacamite, $Cu_2(OH)_3Cl$.

The spectrum obtained for the chloride patina after 128 d of exposure to acid rain (**Figure 3f**) was very similar to that for the brown patina, further showing that brochantite, $Cu_4(SO_4)(OH)_6$, was also formed (reference in **Table 2**).

It was shown that the bronze and artificial patinas underwent changes under stagnant conditions, i.e., a transformation to sulphate minerals. Products such as posnjakite or langite are predominantly precursors for brochantite as the final product. This had previously been reported and demonstrated in the literature.[23]

Table 2: RRUFF references for the Raman peaks shown in **Figure 3**

Antlerite (cm^{-1}) (R050212)	Brochantite (cm^{-1}) (R060117)	Posnjakite (cm^{-1}) (R110172)	Langite (cm^{-1}) (R060090)	Atacamite (cm^{-1}) (R050098)
260	153	183	238	141
343	190	206	434	354
422	242	247	484	444
480	319	335	608	508
607	387	441	764	585
866	423	499	970	814
989	479	607	1068	905
1080	599	976	3394	970
1139	728	1053	3493	3205
1174	773	1112	3570	3343
3490	908	1147		3435
3581	971	3274		
	1097	3415		
	1124	3548		
	3258			
	3397			
	3573			

3.2 Electrochemical measurements

Electrochemical measurements of the open circuit potential (OCP) of the bare, sulphide-patinated and chloride-patinated bronze are shown in **Figure 4a**. Similarly, linear polarization (LP) measurements are shown in **Figure 4b**. Potentiodynamic (PD) curves are shown in **Figure 5**. The values of corrosion potential, E_{corr}, obtained from the OCP measurements, corrosion resistance, R_p, with the protection efficiency calculated from the LP measurements, and corrosion current density, j_{corr}, obtained from the PD measurements, are shown in **Table 3**. The E_{corr} value of the bronze in the urban rain solution was 21.5 mV. The E_{corr} values for the protected bronze samples were negative, being –107 mV and –14.6 mV for Incralac and FA-MS, respectively. The measurements (**Figure 4b**) show that the bronze protected with FA-MS had a polarisation resistance, R_p value of 571 kΩ·cm^2,

which is about 100 times greater than that of the unprotected sample (5.46 kΩ·cm^2). The sample protected with Incralac had the corrosion resistance 3 decades higher, 365 MΩ·cm^2.

The corrosion potential of sulphide-patinated bronze was more negative than the bare bronze and the R_p value (4.88 kΩ·cm^2) was smaller (bare bronze: 5.46 kΩ·cm^2). The E_{corr} values for sulphide-patinated bronze were similar, with the lowest value, –56.6 mV, observed for the sample protected with Incralac. The corrosion resistance of both coated samples was higher than that of the unprotected one, about 200 times greater for FA-MS and 7500 times greater for Incralac. This resulted in high protection efficiencies of 99.5 % and 100 % for FA-MS and Incralac, respectively.

Compared to the sulphide patina and bare bronze, the polarisation resistance of the green chloride patina was lower, 3.36 kΩ·cm^2, (**Table 3**), indicating very unstable corrosion properties. Application of the FA-MS protective coating increased the E_{corr} values, with the corrosion resistance of the protected sample representing a protection efficiency of 71.0 %. Conversely, the E_{corr} values decreased for the sample coated with Incralac, and the protection efficiency remained high, 99.9 %.

PD curves were also obtained, as shown in **Figure 5**. It can be seen that the lowest corrosion current densities were observed on the samples protected with Incralac.

On bare bronze, the FA-MS protection primarily affected the cathodic process, while Incralac showed good barrier properties, as can be observed from the cathodic and anodic PD curves. Similarly, j_{corr} was the lowest in
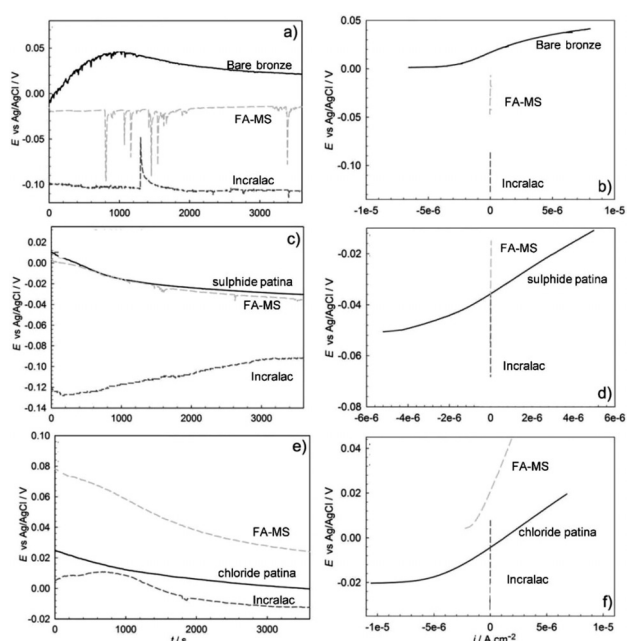
Figure 4: Measurements for the samples with and without a protective coating: a) OCP – bare bronze, b) LP – bare bronze, c) OCP – sulphide-patinated bronze, d) LP – sulphide-patinated bronze, e) OCP – chloride-patinated bronze, f) LP – chloride-patinated bronze

Table 3: Corrosion potential, E_{corr}, corrosion resistance, R_p, and corrosion current density, j_{corr}, with the protection efficiency, *PE,* calculated for each sample measured

Sample	E_{corr} /mV	R_p /(kΩ·cm²)	j_{corr}/(nA/cm²)	*PE*/%
Bronze	21.5	5.46	3 401	—
Bronze – FA-MS	−14.6	571	59.5	99.0
Bronze – Incralac	−107	365 000	0.158	100
Sulphide patina	−30.4	4.88	5 440	—
Sulphide patina – FA-MS	−34.9	942	39.0	99.5
Sulphide patina – Incralac	−56.6	37 500	1.02	100
Chloride patina	−0.32	3.36	6 520	—
Chloride patina – FA-MS	24.0	11.6	4 640	71.0
Chloride patina – Incralac	−12.3	2 600	106	99.9

the case of the sample protected with Incralac, with a value of 0.158 nA/cm².

Application of FA-MS and Incralac on the sulphide bronze changed the cathodic and anodic behaviour, especially in the case of Incralac. The j_{corr} values were low in both cases, 39.0 nA/cm² and 1.02 nA/cm² for the FA-MS and Incralac coatings, respectively.

The application of the FA-MS coating only slightly affected the anodic behaviour of the chloride patina, which was further confirmed by its poor protection efficiency, as estimated from the R_p values, and high corrosion current density, shown by its j_{corr} value of 4.6 μA/cm² (**Table 3**).

Although the Incralac protection showed excellent efficiency and barrier properties, it is known from both the literature[9] and practice[22] that it degrades very quickly upon exposure to an aggressive environment. The newly developed FA-MS coating provided a protection efficiency of 99 % on bare bronze, 99.5 % on brown patinated bronze and 71 % on chloride-patinated bronze. This is a promising result for the protection of bare and brown patinated bronze, while some future adjustments should be made for the green patina. The lower efficiency is most probably a result of the very thick and inhomogeneous structure of the chloride green patina. Such an effect was already observed in previous research studies on various patinated surfaces.[15]

3.3 Contact angle and colour variations

Contact angles of both the unprotected and protected samples are shown in **Table 4.** The samples protected with Incralac have contact angles of around 72°. In the case of the sulphide- and chloride-patinated bronzes, this value is lower than that of the unprotected sample. Of all the samples evaluated, the highest contact angles were observed on those protected with FA-MS, with values of 117°, 115° and 138° for the bare, sulphide-patinated and chloride-patinated bronze, respectively.

The colour differences measured are also shown in **Table 4**. On the non-patinated bronze, the changes in colour were similar after the application of each type of protection: both samples became yellowish, with high Δb^* values of 6.70 and 8.57 for Incralac and FA-MS, respectively. A greater change in colour was detected on the sulphide-patinated bronze, with a ΔE_{ab}^* value of 13.9 for the Incralac coating and a slightly lower value of 11.1 for the FA-MS coating. The changes were noticeable, as the samples had visibly darkened, confirmed by large
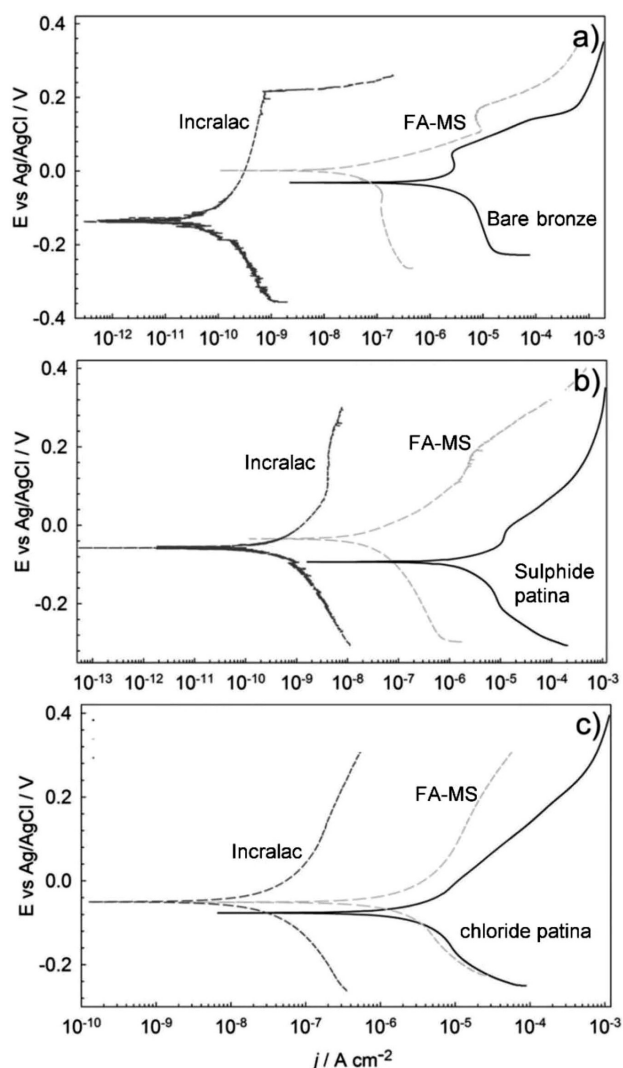
Figure 5: Potentiodynamic curves for the samples with and without protection: a) bare bronze, b) sulphide-patinated bronze, c) chloride-patinated bronze

Table 4: Contact angles of all the samples alongside standard deviations and colour differences, ΔL^*, Δa^*, Δb^* ΔE_{ab}^*, between the unprotected and protected samples

Sample	Contact angle (°) with standard deviation	ΔL^*	Δa^*	Δb^*	ΔE_{ab}^*
Bronze	67 ± 1	—	—	—	—
Bronze – Incralac	73 ± 0	2.27	2.63	6.70	7.55
Bronze – FA-MS	117 ± 1	0.60	2.67	8.57	8.99
Sulphide patina	95 ± 8	—	—	—	—
Sulphide patina – Incralac	73 ± 0	−13.82	0.99	1.45	13.93
Sulphide patina – FA-MS	115 ± 1	−10.80	2.54	0.19	11.10
Chloride patina	98 ± 8	—	—	—	—
Chloride patina – Incralac	71 ± 3	−4.45	0.89	0.24	4.55
Chloride patina – FA-MS	138 ± 6	−0.92	0.48	0.36	1.10

negative values of ΔL^*. The smallest values were measured on the chloride-patinated bronze. The Incralac coating on chloride bronze had a colour difference value of 4.55, representing a visible change in colour, while with the FA-MS coating it was not possible to perceive the change in colour with the naked eye, since the value of ΔE_{ab}^* (1.10) was lower than three.

4 CONCLUSIONS

The following conclusions can be drawn from this study:

1) Different copper sulphates formed on non-patinated and patinated bronze after 128 d of immersion in simulated urban Ljubljana rain. Posnjakite formed on the non-patinated sample, while brochantite was identified on the sulphide- and chloride-patinated bronze samples. The chloride-patinated sample primarily contained atacamite.
2) Large differences in colour, shown as the yellowing and darkening of the samples, were present on both the bare and sulphide-patinated bronzes regardless of the type of protection, while the application of the FA-MS coating on the chloride-patinated bronze did not change the colour of the surface to the extent that the change would be visible with the naked eye.
3) Contact angles of the samples protected with FA-MS were high, which may have resulted in the protection lasting longer.
4) The FA-MS coating exhibited a protection efficiency of more than 99 % on both bare bronze and brown sulphide-patinated bronze, but was less efficient on the chloride-patinated bronze.

Acknowledgments

5 REFERENCES

[1] J. M. Daehner, K. Lapatin, A. Spinelli, Artistry in Bronze: The Greeks and Their Legacy, J. Paul Getty Museum and the Getty Conservation Institute, Los Angeles 2017

[2] D. MacLeod, Bronze Disease: An Electrochemical Explanation, ICCM Bulletin, 7 (1981) 1, 16–26, doi:10.1179/ICCM.1981.7.1.002

[3] D. A. Scott, A Review of Copper Chlorides and Related Salts in Bronze Corrosion and as Painting Pigments, Stud. in Conserv., 45 (2000) 1, 39–53, doi:10.1179/sic.2000.45.1.39

[4] L. Robbiola, C. Fiaud, S. Pennec, New model of outdoor bronze corrosion and its implications for conservation, ICOM-CC, 1993, 796–802

[5] A. Casanova Municchia, F. Bellatreccia, G. D'Ercoli, S. Lo Mastro, I. Reho, M. A. Ricci, A. Sodo, Characterisation of artificial patinas on bronze sculptures of the Carlo Bilotti Museum (Rome), Appl. Phys. A Mater. Sci. Process., 122 (2016), 1–8, doi:10.1007/S00339-016-0551-4

[6] V. Hayez, V. Costa, J. Guillaume, H. Terryn, A. Hubin, Micro Raman spectroscopy used for the study of corrosion products on copper alloys: Study of the chemical composition of artificial patinas used for restoration purposes, Analyst, 130 (2005), 550–556, doi:10.1039/B419080G

[7] A. H. Zittlau, Q. Shi, J. Boerio-Goates, B. F. Woodfield, J. Majzlan, Thermodynamics of the basic copper sulfates antlerite, posnjakite, and brochantite, Chemie der Erde - Geochemistry, 73 (2013), 39–50, doi:10.1016/J.CHEMER.2012.12.002

[8] P. Letardi, Testing new coatings for outdoor bronze monuments: A methodological overview, Coatings, 11 (2021), 1–16, doi:10.3390/COATINGS11020131

[9] G. Bierwagen, T. J. Shedlosky, K. Stanek, Developing and testing a new generation of protective coatings for outdoor bronze sculpture, Prog. Org. Coatings, 48 (2003), 289–296, doi:10.1016/J.PORGCOAT.2003.07.004

[10] J. Wolfe, R. Grayburn, H. Khanjian, A. Heginbotham, A. Phenix, Deconstructing Incralac: A formulation study of acrylic coatings for the protection of outdoor bronze sculpture, ICOM-CC 18th Triennial Conference, Copenhagen 2017, 1–9

[11] C. J. McNamara, M. Breuker, M. Helms, T. D. Perry, R. Mitchell, Biodeterioration of Incralac used for the protection of bronze monuments, J. Cult. Herit., 5 (2004), 361–364, doi:10.1016/J.CULHER.2004.06.002

[12] D. A. Scott, Copper and Bronze in Art: Corrosion, Colorants, Conservation, Getty Publications, LA, California 2002

[13] M. Mihelčič, M. Gaberšček, M. Salzano de Luna, M. Lavorgna, C. Giuliani, G. Di Carlo, A. K. Surca, Effect of silsesquioxane addition on the protective performance of fluoropolymer coatings for bronze surfaces, Mater. Des., 178 (2019), 1–13, doi:10.1016/J.MATDES.2019.107860

[14] T. Kosec, L. Škrlep, E. Švara Fabjan, A. Sever Škapin, G. Masi, E. Bernardi, C. Chiavari, C. Josse, J. Esvan, L. Robbiola, Development of multi-component fluoropolymer based coating on simulated outdoor patina on quaternary bronze, Prog. Org. Coatings, 131 (2019), 27–35, doi:10.1016/J.PORGCOAT.2019.01.040

[15] T. Kosec, Ž. Novak, E. Š. Fabjan, L. Škrlep, A. Sever Škapin, P. Ropret, Corrosion protection of brown and green patinated bronze, Prog. Org. Coatings, 161 (2021), 1–9, doi:10.1016/J.PORGCOAT.2021.106510

[16] J. Wang, Y. Wu, S. Zhang, A new coating system modified with nano-sized particles for archaeological bronze protection, Stud. Conserv., 59 (2014), 268–275, doi:10.1179/2047058414Y.0000000135

[17] T. Kosec, Ž. Novak, E. Švara Fabjan, L. Škrlep, M. Finšgar, Exploring the protection mechanism of a combined fluoropolymer coating on sulphide patinated bronze, Prog. Org. Coatings, 172 (2022), 1–13, doi:10.1016/j.porgcoat.2022.107071

[18] P. A. Schweitzer, Fundamentals of Metallic Corrosion: Atmospheric and Media Corrosion of Metals, 2nd ed., CRC Press/Taylor & Francis Group, Boca Raton 2007

[19] M. Del Mar Pérez, A. Saleh, A. Yebra, R. Pulgar, Study of the variation between CIELAB ΔE^* and CIEDE2000 color-differences of resin composites, Dent. Mater. J., 26 (2007), 21–28, doi:10.4012/DMJ.26.21

[20] K. Marušić, H. Otmačić-Ćurković, Š. Horvat-Kurbegović, H. Takenouti, E. Stupnišek-Lisac, Comparative studies of chemical and electrochemical preparation of artificial bronze patinas and their protection by corrosion inhibitor, Electrochim. Acta, 54 (2009), 7106–7113, doi:10.1016/J.ELECTACTA.2009.07.014

[21] G. Niaura, Surface-enhanced Raman spectroscopic observation of two kinds of adsorbed OH- ions at copper electrode, Electrochim. Acta, 45 (2000), 3507–3519, doi:10.1016/S0013-4686(00)00434-5

[22] P. Ropret, T. Kosec, Raman investigation of artificial patinas on recent bronze – Part I: climatic chamber exposure, J. Raman Spectrosc., 43 (2012), 1578–1586, doi:10.1002/JRS.4068

[23] V. Hayez, J. Guillaume, A. Hubin, H. Terryn, Micro-Raman spectroscopy for the study of corrosion products on copper alloys: setting up of a reference database and studying works of art, J. Raman Spectrosc., 35 (2004), 732–738, doi:10.1002/JRS.1194